

See discussions, stats, and author profiles for this publication at: <https://www.researchgate.net/publication/44661726>

Synthesis and Application of Widely Soluble Graphene Sheets

ARTICLE *in* LANGMUIR · JULY 2010

Impact Factor: 4.46 · DOI: 10.1021/la101534n · Source: PubMed

CITATIONS

104

READS

12

6 AUTHORS, INCLUDING:



Li Niu

Chinese Academy of Sciences

214 PUBLICATIONS 7,032 CITATIONS

SEE PROFILE

Synthesis and Application of Widely Soluble Graphene Sheets

Fenghua Li, Yu Bao, Jia Chai, Qixian Zhang, Dongxue Han, and Li Niu*

Engineering Laboratory for Modern Analytical Techniques, c/o State Key Laboratory of Electroanalytical Chemistry, Changchun Institute of Applied Chemistry, and Graduate University of the Chinese Academy of Sciences, Chinese Academy of Sciences, Changchun 130022, PR China

Received April 17, 2010. Revised Manuscript Received May 25, 2010

A widely soluble graphene sheet/Congo red (GSCR) composite was synthesized and applied to prepare GSCR/Au hybrid materials. UV-vis absorption, Fourier transform infrared, Raman, and X-ray photoelectron spectra revealed that Congo red (CR) is successfully coupled on graphene sheets. The morphology of GSCR was studied by transmission electron microscopy, scanning electron microscopy, and atomic force microscopy. The dispersion behavior of the GSCR composite was also studied in 18 different solvents, and the digital images indicate that it is soluble both in water and in a variety of organic solvents. The GSCR nanosheets are still single layers or bilayers in water and individual from one to another after 100 days of storage. Furthermore, the mechanism of GSCR's good solubility was successfully explained by the Hansen solubility parameters. The four standard probe result shows that the GSCR films have a bulk conductivity of $\sim 6850 \text{ S m}^{-1}$. The wide solubility and long lifetime of GSCR solutions are absolutely necessary for further treatment. As an example, Au nanoparticles densely decorated CR-functionalized graphene sheets through electrostatic interaction.

1. Introduction

Graphene, a single-atom-thick sheet of hexagonally arrayed sp^2 -bonded carbon atoms, has attracted tremendous attention from both experimental and theoretical communities in recent years.¹ The unique electronic properties of graphene sheets² provide potential applications in synthesizing nanocomposites^{3,4} and fabricating field-effect transistors,⁵ dye-sensitized solar cells,⁶ lithium ion batteries,⁷ electromechanical resonators,⁸ and electrochemical sensors.^{9,10} However, just as for the other newly discovered allotropes of carbon (fullerenes and carbon nanotubes), material availability and processability will be the rate-limiting steps in the evaluation of putative applications of graphene. For graphene, that availability is encumbered by having to surmount the high cohesive van der Waals energy (5.9 kJ mol^{-1}) adhering graphitic sheets to one another.¹¹ Some methods have been used to prepare individual graphene sheets and to improve the properties of graphene. These methods include a scotch tape (peel off) method,¹² epitaxial growth,¹³ chemical vapor

deposition,¹⁴ the solvothermal reduction of graphene oxide,¹⁵ the electrochemical reduction of graphene oxide,¹⁶ and the chemical reduction of graphene oxide.¹⁷

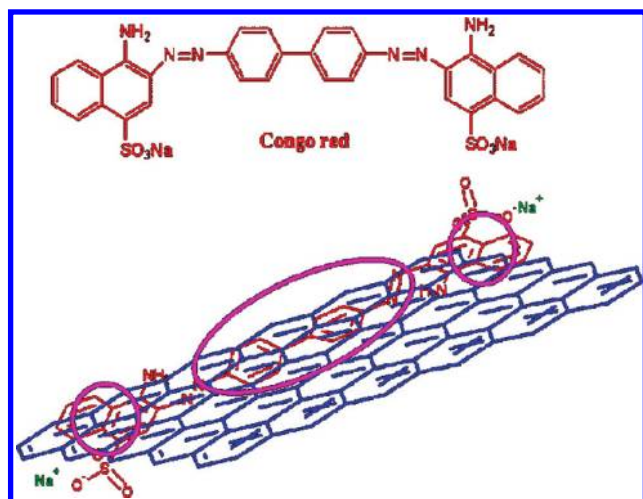
Water-soluble graphene sheets have already been prepared and applied in some fields through these efforts. The chemically converted graphene sheets (GS) prepared by using hydrazine as a reducing agent were well dispersed in water because of the electrostatic repulsion of negatively charged carboxylic groups.¹⁸ Stable graphene suspensions could be also prepared by heating a graphite oxide (GO) suspension under strongly alkaline conditions.¹⁹ Strong bases can confer large negative charges through reactions with reactive hydroxyl, epoxy, and carboxylic acid groups on the GO sheets. Water-soluble aromatic electroactive dye methylene green was used as a stabilizer to prepare stable aqueous dispersions of graphene sheets through the Coulombic repulsion.²⁰ The electrostatic repulsion of negatively charged sulfonic groups on the graphene surface was also utilized to disperse graphene sheets in water.²¹ Moreover, polymer-coated graphene sheets, such as polyvinylpyrrolidone and sulfonated polyaniline, were dispersed well in an aqueous solution.^{22,23} Meanwhile, the use of organic solvents as media for dispersing graphene sheets has also been addressed. Aryl diazonium salt-modified graphene sheets could be dispersed in *N,N*-dimethylformamide (DMF) by varying the aryl addends.²⁴ Graphene oxide reduced by *N,N*-dimethylhydrazine in DMF

*Corresponding author. Tel: +86-431-8526 2425. Fax: +86-431-8526 2800. E-mail: lniu@ciac.jl.cn.

- (1) Allen, M. J.; Tung, V. C.; Kaner, R. B. *Chem. Rev.* **2010**, *110*, 132–145.
- (2) Eda, G.; Chhowalla, M. *Nano Lett.* **2009**, *9*, 814–818.
- (3) Li, F.; Song, J.; Yang, H.; Gan, S.; Zhang, Q.; Han, D.; Ivaska, A.; Niu, L. *Nanotechnology* **2009**, *20*, 455602.
- (4) Li, F.; Yang, H.; Shan, C.; Zhang, Q.; Han, D.; Ivaska, A.; Niu, L. *J. Mater. Chem.* **2009**, *19*, 4022–4025.
- (5) Li, X.; Wang, X.; Zhang, L.; Lee, S.; Dai, H. *Science* **2008**, *319*, 1229–1232.
- (6) Hong, W.; Xu, Y.; Lu, G.; Li, C.; Shi, G. *Electrochem. Commun.* **2008**, *10*, 1555–1558.
- (7) Yoo, E.; Kim, J.; Hosono, E.; Zhou, H.-s.; Kudo, T.; Honma, I. *Nano Lett.* **2008**, *8*, 2277–2282.
- (8) Bunch, J. S.; van der Zande, A. M.; Verbridge, S. S.; Frank, I. W.; Tanenbaum, D. M.; Parpia, J. M.; Craighead, H. G.; McEuen, P. L. *Science* **2007**, *315*, 490–493.
- (9) Shan, C.; Yang, H.; Han, D.; Zhang, Q.; Ivaska, A.; Niu, L. *Langmuir* **2009**, *25*, 12030–12033.
- (10) Zhu, C.; Guo, S.; Zhai, Y.; Dong, S. *Langmuir* **2010**, *26*, 7614–7618.
- (11) Zacharia, R.; Ulbricht, H.; Hertel, T. *Phys. Rev. B* **2004**, *69*, 155406.
- (12) Novoselov, K. S.; Geim, A. K.; Morozov, S. V.; Jiang, D.; Zhang, Y.; Dubonos, S. V.; Grigorieva, I. V.; Firsov, A. A. *Science* **2004**, *306*, 666–669.
- (13) Berger, C.; Song, Z.; Li, X.; Wu, X.; Brown, N.; Naud, C.; Mayou, D.; Li, T.; Hass, J.; Marchenkov, A. N.; Conrad, E. H.; First, P. N.; de Heer, W. A. *Science* **2006**, *312*, 1191–1196.
- (14) Wang, J. J.; Zhu, M. Y.; Outlaw, R. A.; Zhao, X.; Manos, D. M.; Holloway, B. C. *Carbon* **2004**, *42*, 2867–2872.

- (15) Nethravathi, C.; Rajamathi, M. *Carbon* **2008**, *46*, 1994–1998.
- (16) Wang, Z.; Zhou, X.; Zhang, J.; Boey, F.; Zhang, H. *J. Phys. Chem. C* **2009**, *113*, 14071–14075.
- (17) Wang, G.; Yang, J.; Park, J.; Gou, X.; Wang, B.; Liu, H.; Yao, J. *J. Phys. Chem. C* **2008**, *112*, 8192–8195.
- (18) Li, D.; Müller, M. B.; Gilje, S.; Kaner, R. B.; Wallace, G. G. *Nat. Nanotechnol.* **2008**, *3*, 101–105.
- (19) Fan, X.; Peng, W.; Li, Y.; Li, X.; Wang, S.; Zhang, G.; Zhang, F. *Adv. Mater.* **2008**, *20*, 4490–4493.
- (20) Liu, H.; Gao, J.; Xue, M.; Zhu, N.; Zhang, M.; Cao, T. *Langmuir* **2009**, *25*, 12006–12010.
- (21) Si, Y.; Samulski, E. T. *Nano Lett.* **2008**, *8*, 1679–1682.
- (22) Bourlinos, A. B.; Georgakilas, V.; Zboril, R.; Steriotis, T. A.; Stubos, A. K.; Trapalis, C. *Solid State Commun.* **2009**, *149*, 2172–2176.
- (23) Bai, H.; Xu, Y.; Zhao, L.; Li, C.; Shi, G. *Chem. Commun.* **2009**, 1667–1669.
- (24) Lomeda, J. R.; Doyle, C. D.; Kosynkin, D. V.; Hwang, W.-F.; Tour, J. M. *J. Am. Chem. Soc.* **2008**, *130*, 16201–16206.

Scheme 1. Structure of CR and the Reaction Mechanism between CR and Graphene Sheets



and *N*-methyl-2-pyrrolidone (NMP) could also yield graphene dispersions in organic media.²⁵ Furthermore, graphene sheets functionalized by azomethine ylide and the 7,7,8,8-tetracyanoquinodimethane anion were all dispersible in several highly polar organic solvents and water.^{26,27} Another kind of graphene covalently grafted to a polystyrene-polyacrylamide copolymer was dispersed only in water and xylene.²⁸ With the exception of these functionalized graphenes, graphite could be directly exfoliated to multilayer structures in NMP at a relatively low concentration (~ 0.01 mg/mL).²⁹ In addition, a peculiar class of perfluorinated organic solvents were also used to prepare organically soluble graphene by liquid-phase exfoliation graphite.³⁰

It is worth noting that graphene sheets without modification have been dispersed in some mixtures of tested solvents/DMF/H₂O.³¹ Amphiphilic graphite oxide grafted to an oligoester via toluene diisocyanate has also been synthesized.³² It is regrettable that widely soluble graphene sheets have rarely been addressed. In this article, a kind of widely soluble graphene sheet was synthesized by functionalizing graphene sheets with Congo red (CR). The structure of CR and the reaction mechanism between CR and graphene sheets are shown in Scheme 1. The CR molecules were coupled on graphene sheets through the π - π interactions between the aniline moieties of CR and the aromatic rings of graphene, which was highlighted by pink circles in Scheme 1. The highest solubility of the resulting graphene sheets/Congo red (GSCR) composite is 7.5 mg/mL in water. Moreover, the resulting GSCR composite can also be dispersed in various organic solvents. The GSCR aqueous solution and the DMF solution can be stably stored for 100 days and 2 weeks, respectively. In a word, the wide solubility and long lifetime of GSCR solutions are absolutely necessary for further treatment. A kind of GSCR/Au hybrid material was successfully synthesized as an example.

2. Experimental Section

2.1. Materials. Graphite powder (spectral requirement, Shanghai Chemicals, China), hydrazine solution (50% in water, Beijing Yili Chemicals, China), ammonia solution (25% in water, Beijing Chemicals, China), CR (99%, Shanghai Yuanhang Chemicals, China), H₂AuCl₄·4H₂O (98%, Shanghai Chemicals, China), 3-bromopropylamine hydrobromide (98%, Aldrich), poly(diallyldimethylammonium chloride) (PDDA, 20 wt % in water, Aldrich), and 1-methylimidazole (98%, Linhai Kaile Chemicals, China) were distilled at reduced pressure before use. All chemicals were of analytical-grade quality and used as received except for special statements. All aqueous solutions were prepared with ultrapure water (>18 M Ω cm) obtained from a Milli-Q Plus system (Millipore).

2.2. Preparation of GO and GS. GO was synthesized from natural graphite powder by a modified Hummers method as originally presented by Kovtyukhova and colleagues.³³ GS was synthesized by the method presented by Li et al.¹⁸ The detailed processes are shown in the Supporting Information.

2.3. Synthesis of GSCR. In a typical preparation procedure for the GSCR composite, 5 mg of CR was added to 40 mL of the above GS solution and then stirred at 50 °C overnight. The product was subsequently filtered through a nylon membrane with 0.22 μ m pores and washed with water until the filtrate became colorless. The GSCR composite was dried at room temperature. To prepare GSCR solutions, the dried GSCR nanocomposite was dispersed in tested organic solvents by ultrasonication for 15 min. Digital photographs were taken after 24 h and 100 days of sedimentation at room temperature. The aqueous solution was distributed by using distilled water, and all of the tested organic solvents were untreated before they were used.

2.4. Synthesis of the GSCR/Au Nanoparticle Composite. Ionic-liquid-stabilized Au nanoparticles (Au-IL) were prepared following our previous report.³⁴ Au-ILs (2 mg) were dispersed in 2 mL of GSCR solution by ultrasonication. The resulting solution was stirred for 10 h at room temperature. GSCR/Au was washed several times with ultrapure water and collected by centrifugation and dried under vacuum at room temperature. Meanwhile, the GS/Au composite was prepared in the same way, except that the GS solution was used to replace the GSCR solution.

2.5. Characterization. UV-vis absorption spectra were recorded using a Cary 500 UV/vis/near-IR spectrometer. Fourier transform infrared spectra (FTIR) were recorded using a Bruker Tensor 27 spectrometer. Raman spectra were collected using a Renishaw 2000 system with an argon ion laser (514.5 nm) and a charge-coupled-device detector. X-ray photoelectron spectra (XPS) analysis was carried out on an Escalab MK II X-ray photoelectron spectrometer. Transmission electron microscopy (TEM) images were obtained using a FEI Tecnai G² transmission electron microscope operating at 200 kV and a Hitachi-600 transmission electron microscope operating at 100 kV. Scanning electron microscopy (SEM) images were conducted with an XL30 ESEM FEG field emission scanning electron microscope. Digital photographs were taken with a Canon 570 camera. Atomic force microscope (AFM) studies were performed on a commercial scanning probe microscope (SPA300HV, with an SPI3800N Probe Station, Seiko Instruments Inc., Japan). The tapping modes were used to study the surface structure. Silicon tips with a frequency of 63–70 kHz and a spring constant of 2 N/m were used. The AFM sample was fabricated by a self-assembled method. Briefly, the cleaned silicon wafer was put in 1.0% PDDA solution for 20 min to form a positively charged surface, and then it was taken out, washed with water three times, and dried in a stream of ultrapure N₂. The substrate was then soaked in a GSCR dispersion for 20 min, rinsed, and dried again. The square resistance was measured under ambient conditions by a standard four-probe method. A Keithley 2400 source meter and a Keithley

(25) Villar-Rodil, S.; Paredes, J. I.; Martínez-Alonso, A.; Tascón, J. M. D. *J. Mater. Chem.* **2009**, *19*, 3591–3593.

(26) Georgakilas, V.; Bourlino, A. B.; Zboril, R.; Steriotis, T. A.; Dallas, P.; Stubos, A. K.; Trapalis, C. *Chem. Commun.* **2010**, *46*, 1766–1768.

(27) Hao, R.; Qian, W.; Zhang, L.; Hou, Y. *Chem. Commun.* **2008**, 6576–6578.

(28) Shen, J.; Hu, Y.; Li, C.; Qin, C.; Ye, M. *Small* **2009**, *5*, 82–85.

(29) Hernandez, Y.; Nicolosi, V.; Lotya, M.; Blighe, F. M.; Sun, Z.; De, S.; McGovern, I. T.; Holland, B.; Byrne, M.; Gun'ko, Y. K.; Boland, J. J.; Niraj, P.; Duesberg, G.; Krishnamurthy, S.; Goodhue, R.; Hutchison, J.; Scardaci, V.; Ferrari, A. C.; Coleman, J. N. *Nat. Nanotechnol.* **2008**, *3*, 563–568.

(30) Bourlino, A. B.; Georgakilas, V.; Zboril, R.; Steriotis, T. A.; Stubos, A. K. *Small* **2009**, *5*, 1841–1845.

(31) Park, S.; An, J.; Jung, I.; Piner, R. D.; An, S. J.; Li, X.; Velamakanni, A.; Ruoff, R. S. *Nano Lett.* **2009**, *9*, 1593–1597.

(32) Xu, C.; Wu, X.; Zhu, J.; Wang, X. *Carbon* **2008**, *46*, 386–389.

(33) Kovtyukhova, N. I.; Ollivier, P. J.; Martin, B. R.; Mallouk, T. E.; Chizhik, S. A.; Buzaneva, E. V.; Gorchinskiy, A. D. *Chem. Mater.* **1999**, *11*, 771–778.

(34) Wang, Z.; Zhang, Y.; Zhang, Q.; Shen, Y.; Kuehner, D.; Ivaska, A.; Niu, L. *Green Chem.* **2008**, *10*, 907–909.

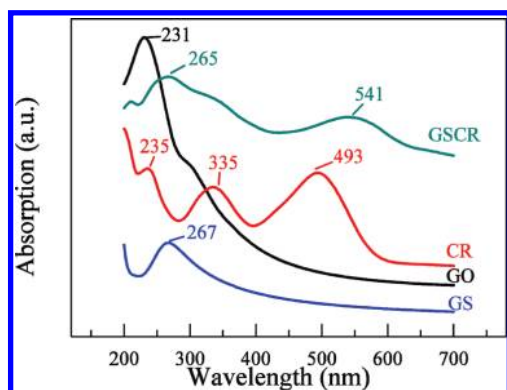


Figure 1. UV-vis absorption of GO, GS, CR, and GSCR composites.

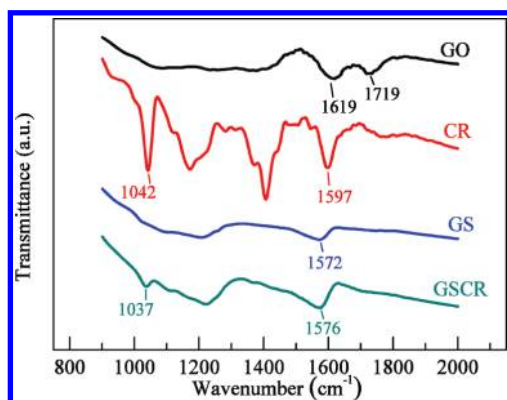


Figure 2. FTIR spectra of GO, GS, CR, and GSCR composites.

2000 multimeter (Keithley Instruments, Cleveland, OH) were connected to the sample. Four electrode contacts with an interelectrode spacing of 1.0 mm were formed on a 0.1-mm-thick sample with a 2 cm diameter. The sample was prepared by a vacuum filtration strategy using an Al_2O_3 membrane with 0.22 μm pores.

3. Results and Discussion

3.1. Spectral Characterization of the GSCR Composite.

Figure 1 shows the UV-vis absorption spectra of GO, GS, CR, and GSCR dispersions. The spectrum obtained for the GO dispersion (black line) exhibits a maximum at 231 nm (attributed to $\pi-\pi^*$ transitions of aromatic C=C bonds) and a shoulder at about 300 nm (ascribed to $n-\pi^*$ transitions of C=O bonds). After reduction (blue line), the aromatic C=C bonds red shift to 267 nm, indicating the restoration of a π -conjugation network within GS.¹⁸ In a CR aqueous solution, three well-defined peaks situated at 235, 335, and 493 nm (red line) are attributed to the short-wavelength $\Phi-\Phi^*$ transitions and the long-wavelength $\pi-\pi^*$ transitions of the aromatic rings and the $n-\pi^*$ transitions of the free electron pairs of the N atoms of the azo group, respectively.³⁵ Much different from the CR line, the UV-vis spectrum of GSCR exhibits two new absorptions at ca. 265 and 541 nm (green line). The maximum absorption at 265 nm is ascribed to the π -plasmon absorption of GS.¹⁸ The peak at 541 nm might arise from the charge transfer between the aniline moieties of CR and GS.³⁵ The latter is also direct evidence of the influence of CR $\pi-\pi$ stacking on the electronic structure of GS.

The UV-vis results are corroborated by the FTIR results (Figure 2). For the GO film, the C=O peak in the carboxylic acid and carbonyl moieties is at 1719 cm^{-1} . The peak at 1619 cm^{-1} can be assigned to the vibrations of the residual water but may also

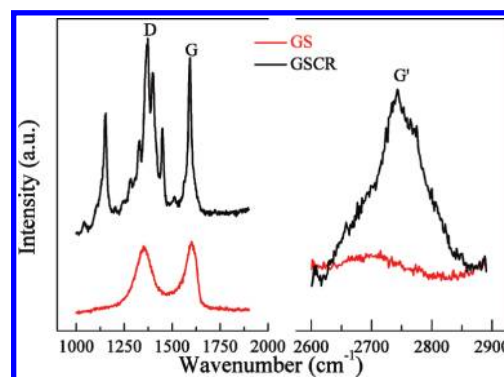


Figure 3. Raman spectra of GS and GSCR composites.

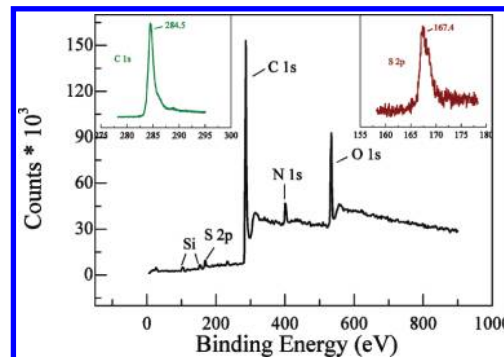


Figure 4. XPS spectrum of GSCR composites. (Insets) Spectra of C 1s (top left) and S 2p (top right).

contain components from skeletal vibrations of unoxidized graphitic domains.³⁶ The absorption of GS in this range is also observable but is not as prominent as that observed for GO. The strong peak at 1572 cm^{-1} is likely due to stretching of the C=C bonds of GS restored upon hydrazine reduction.³⁷ The characteristics of CR are consistent with the previous report.³⁵ The peak at 1042 cm^{-1} is attributed to the stretching vibration of S=O bonds in $-\text{SO}_3^-$.³⁸ As seen from the GSCR spectrum (green line), the S=O stretching vibration in CR is still observed but shifts to a low wavenumber of 1037 cm^{-1} . The red shift might be attributed to the $\pi-\pi$ stacking between GS and CR. The new band at 1576 cm^{-1} might be assigned to the overlapping of the stretching of C=C bonds of GS (1572 cm^{-1}) and that of CR (1597 cm^{-1}).

Figure 3 shows the Raman spectra of GS (red line) and GSCR (black line). The peaks at 1373 and 1592 cm^{-1} ascribed to the D and G bands of graphene are observed in both GS and GSCR.³ With the exception of these, several new bands located at about 1449, 1400, 1332, and 1151 cm^{-1} appear in GSCR because of the characteristic scattering of CR.³⁹ From 2600 to 2900 cm^{-1} , an obvious G' band of graphene is observed at 2743 cm^{-1} in GSCR. It is known that the shape of the G' spectra of graphene changes according to the number of layers.⁴⁰ The single sharp peak of the G' band of GSCR indicates that the GSCR nanosheets are composed of a single layer of graphene sheets.

The composition of the GSCR composite was further confirmed by the XPS result (Figure 4). The composite shows an

(36) Stankovich, S.; Piner, R. D.; Nguyen, S. T.; Ruoff, R. S. *Carbon* **2006**, *44*, 3342–3347.

(37) Titelman, G. I.; Gelman, V.; Bron, S.; Khalfin, R. L.; Cohen, Y.; Bianco-Peled, H. *Carbon* **2005**, *43*, 641–649.

(38) Xu, D.-M.; Zhao, Z.-L.; Wang, A.-F.; Zhang, K.-D.; Zhu, X.-L. *J. Appl. Polym. Sci.* **2008**, *107*, 2578–2583.

(39) Sajid, J.; Elhaddaoui, A.; Turrell, S. J. *Mol. Struct.* **1997**, *408*, 181–184.

(40) Dresselhaus, M. S.; Jorio, A.; Hofmann, M.; Dresselhaus, G.; Saito, R. *Nano Lett.* **2010**, *10*, 751–758.

(35) Hu, C.; Chen, Z.; Shen, A.; Shen, X.; Li, J.; Hu, S. *Carbon* **2006**, *44*, 428–434.

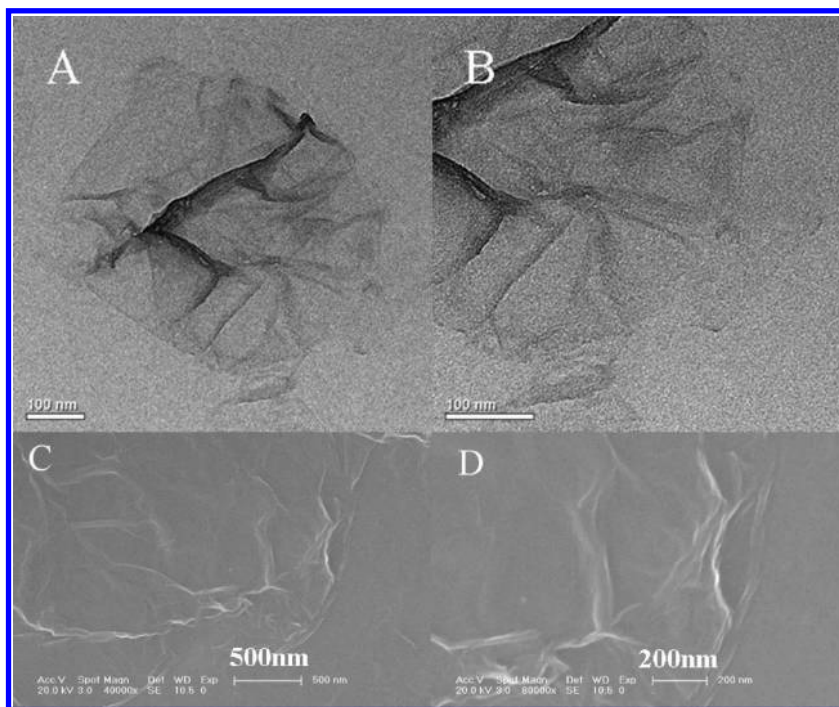


Figure 5. (A, B) TEM and (C, D) SEM images of the GSCR sheets at different magnifications.

obvious C–C peak at 284.5 eV and also exhibits nonobvious oxygen functionalities (top-left inset). It is consistent with the C 1s XPS spectrum of the reduced exfoliated GO in a previous report.⁴¹ The S 2p peak appearing at 167.4 eV (top-right inset) is due to the $-\text{SO}_3^-$ state.⁴² The XPS result is consistent with the results of UV–vis and FTIR spectra.

Figure 5 shows the TEM and SEM images of GSCR sheets. It is easy to see that the GSCR layers are sheets that are several hundreds or thousands of nanometers thick with some pleats. They are transparent and very thin, which can be seen from the fringe of GSCR sheets.

3.2. Dispersive and Conductive Properties of the GSCR Composite. The GSCR composite can be dispersed in a variety of solvents as shown in Figure 6. The upper layers of the GSCR (a) toluene, (b) benzene, and (f) chloroform solutions are all nearly colorless, indicating that the GSCR composite is not dispersed in these three solvents. The solubility of GSCR in (c) tetrahydrofuran (THF), (d) ethyl acetate, (e) isopropanol, (g) acetone, (h) acetonitrile, (m) NMP, (o) isoamyl alcohol, (p) m-cresol, (q) pyridine, and (r) 1,4-dioxane is better because the color of the upper solution becomes dark. It is worth noting that GSCR can be completely dispersed in (i) DMF, (j) methanol, (k) DMSO, (l) water, and (n) ethanol. It is not strange that GSCR is water-soluble because both GS and CR are soluble in water. In contrast, it is of great interest to classify the “dispersing power” for GSCR in those organic solvents. The Hansen solubility parameters are used to explain the dispersive property of GSCR. The Hansen solubility parameters include the dispersion cohesion parameter (δ_d), the polarity cohesion parameter (δ_p), and the hydrogen bonding cohesion parameter (δ_h).⁴³ δ_d , δ_p , and δ_h are attributed to the dispersion interactions, permanent dipolar

molecular interactions, and hydrogen bonding molecular interactions, respectively.⁴⁴ The δ_d , δ_p , and δ_h values for the tested solvents are shown in Table S1. A recent study indicated that polar and hydrogen bonding Hansen parameters are important factors for obtaining reduced graphene oxide dispersions.³¹ Figure 7 shows the three dispersive areas of GSCR divided by the sum of $\delta_p + \delta_h$. The resulting GSCR is not dispersed in solvents with $\delta_p + \delta_h < 8.6$. Meanwhile, in the range of 9.2–24.1, the GSCR is partially dispersed, which might be mainly due to the soluble properties of graphene. The Hansen δ_d , δ_p , and δ_h parameters for graphene are 18.0, 9.3, and 7.7 as reported by the Coleman group.⁴⁵ The value of $\delta_p + \delta_h$ is 17.0, which is consistent with our results. Clearly, good solvents for GSCR have $\delta_p + \delta_h \geq 25.0$. It is reasonable that the exposed $-\text{SO}_3\text{Na}$ groups allow dispersibility in relatively highly polar solvents, even water. Obviously, the introduction of CR enlarges the dispersive area of graphene, which can be further confirmed by comparing the dispersive properties of GSCR with those of graphene sheets. Graphene sheets without modification are more difficult to wet than graphene oxides by water and some other polar solvents because of the decrease in the number of epoxy and hydroxyl groups during the reductive process.⁴⁶ The $-\text{SO}_3\text{Na}$ groups of CR coupled with graphene might remedy the insufficient number of functional groups in graphene sheets. Therefore, the flat placement of the CR on the surface of graphene is absolutely necessary to improve graphene sheets’ dispersive properties.

The storage stability of the GSCR aqueous solution and the DMF solution was also studied. The digital photographs of (a) GSCR in water, (b) GSCR in DMF, (c) GS in water, and (d) GO in water prepared after 24 h (A) and 100 days (B) are shown in Figure 8. A little sediment appears at the bottom of the

(41) Stankovich, S.; Dikin, D. A.; Piner, R. D.; Kohlhaas, K. A.; Kleinhammes, A.; Jia, Y.; Wu, Y.; Nguyen, S. T.; Ruoff, R. S. *Carbon* **2007**, *45*, 1558–1565.

(42) Li, F.; Wang, Z.; Shan, C.; Song, J.; Han, D.; Niu, L. *Biosens. Bioelectron.* **2009**, *24*, 1765–1770.

(43) Hansen, C. M. *Hansen Solubility Parameters: A User's Handbook*, 2nd ed.; CRC Press: Boca Raton, FL, 2007.

(44) Bergin, S. D.; Sun, Z.; Rickard, D.; Streich, P. V.; Hamilton, J. P.; Coleman, J. N. *ACS Nano* **2009**, *3*, 2340–2350.

(45) Hernandez, Y.; Lotya, M.; Rickard, D.; Bergin, S. D.; Coleman, J. N. *Langmuir* **2010**, *26*, 3208–3213.

(46) Wang, S.; Zhang, Y.; Abidi, N.; Cabrales, L. *Langmuir* **2009**, *25*, 11078–11081.

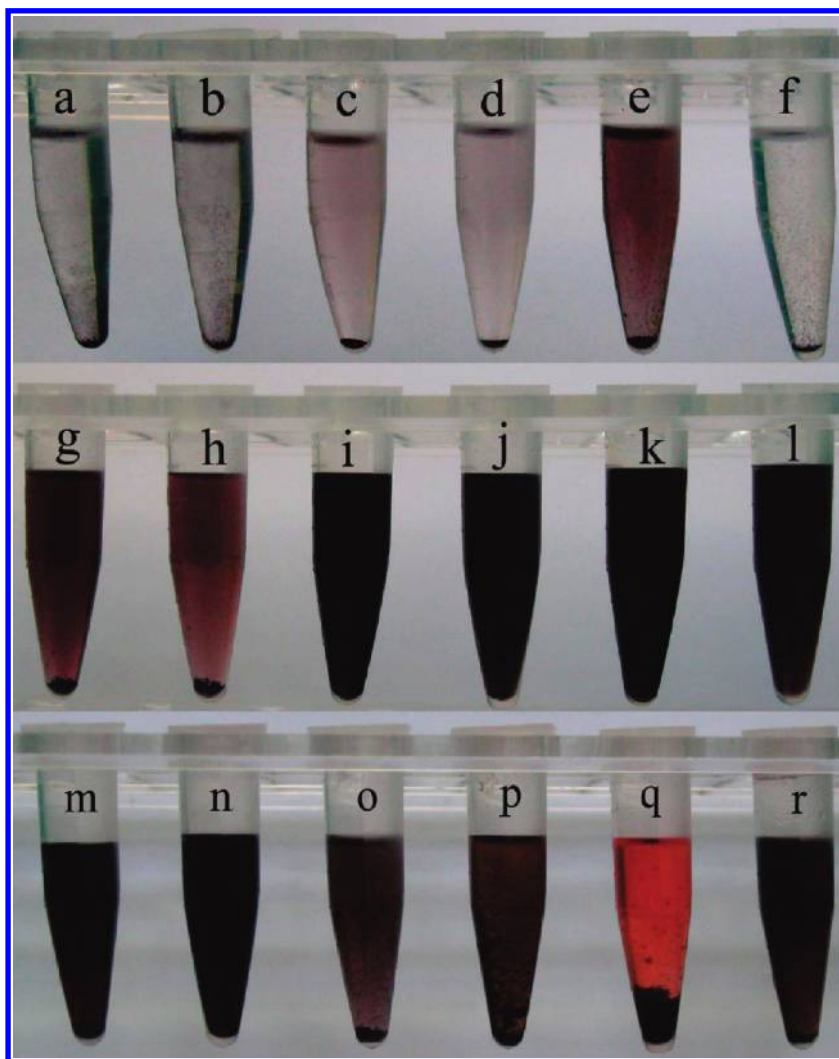


Figure 6. Digital photographs of GSCR nanocomposites in (a) toluene, (b) benzene, (c) THF, (d) ethyl acetate, (e) isopropanol, (f) chloroform, (g) acetone, (h) acetonitrile, (i) DMF, (j) methanol, (k) DMSO, (l) water, (m) NMP, (n) ethanol, (o) isoamyl alcohol, (p) m-cresol, (q) pyridine, and (r) 1,4-dioxane. The preparing concentration of all of the above solutions is about 0.5 mg/mL with 24 h of sedimentation after vigorous vibration.

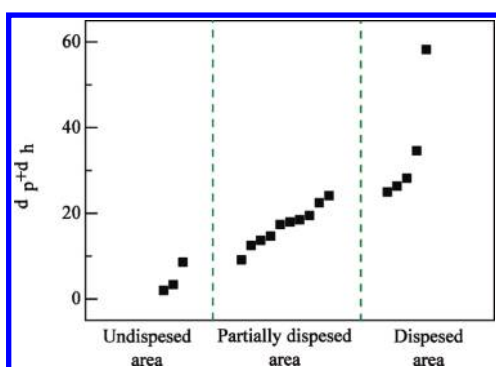


Figure 7. Dispersive behaviors of GSCR with $\delta_p + \delta_h$.

GSCR DMF solution tube (A (b)) because the preparing concentration is the same as that for the GSCR aqueous solution (A (a)). After 100 days of storage, there is still no sediment in the GSCR aqueous solution (B (a)). The GSCR DMF solution was not stable as long as the GSCR water solution. Comparing with A (b), we can see that more sediment appears at the bottom of tubes and that the color of the solution becomes weaker in B (b). The lifetime of the GSCR DMF

solution is 2 weeks, which is long enough for further treatment. However, after 100 days, GS aggregated and its upper solution became colorless in the GS aqueous solution (B (c)).

The good storage properties of the GSCR aqueous solution is further confirmed by the AFM image. Figure 9(A) shows the AFM image of GSCR self-assembled onto a silicon wafer. The theoretical height for a graphene sheet functionalized on both sides is ca. 2.2 nm, assuming that the height of the bare graphene sheets is 1 nm⁴⁷ with the substituted aromatic groups contributing ca. 0.6 nm to the height.²⁴ On average, the height of a GSCR single layer ranges from 1.5 to 2.0 nm. The few very high places might be attributed to the overlapped or turn-up edges. The small dotlike structures on the surface of the silicon substrate are attributed to the accumulation of PDDA from the sample fabrication and particles of inorganic salts that are leftover from the preparation of GO.³⁶ Overall, the GSCR nanosheets are mainly composed of single or bilayers of graphene sheets over 3 months. It is also confirmed by the (B) TEM and (C) SEM results. The thin sheets are still transparent and retain their primary morphologies. The reason for the long lifetime of the GSCR

(47) Stankovich, S.; Piner, R. D.; Chen, X.; Wu, N.; Nguyen, S. T.; Ruoff, R. S. *J. Mater. Chem.* **2006**, *16*, 155–158.

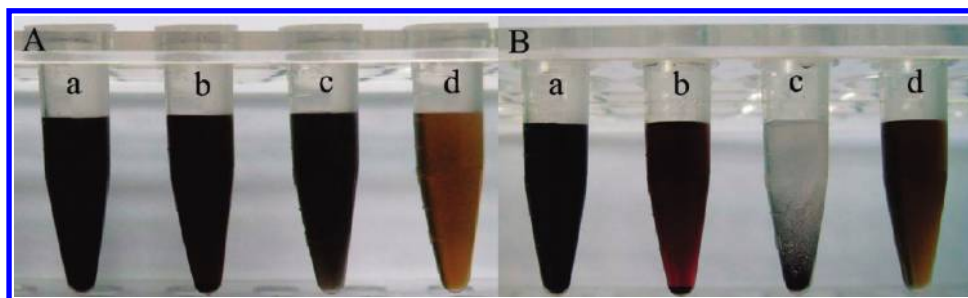


Figure 8. (A) Digital photographs of 24 h of sedimentation after vigorous vibration for (a) GSCR in water (2.0 mg/mL), (b) GSCR in DMF, (c) GS in water (0.25 mg/mL), and (d) GO in water (0.25 mg/mL). (B) Digital photographs of the same solution after 100 days of storage at room temperature.

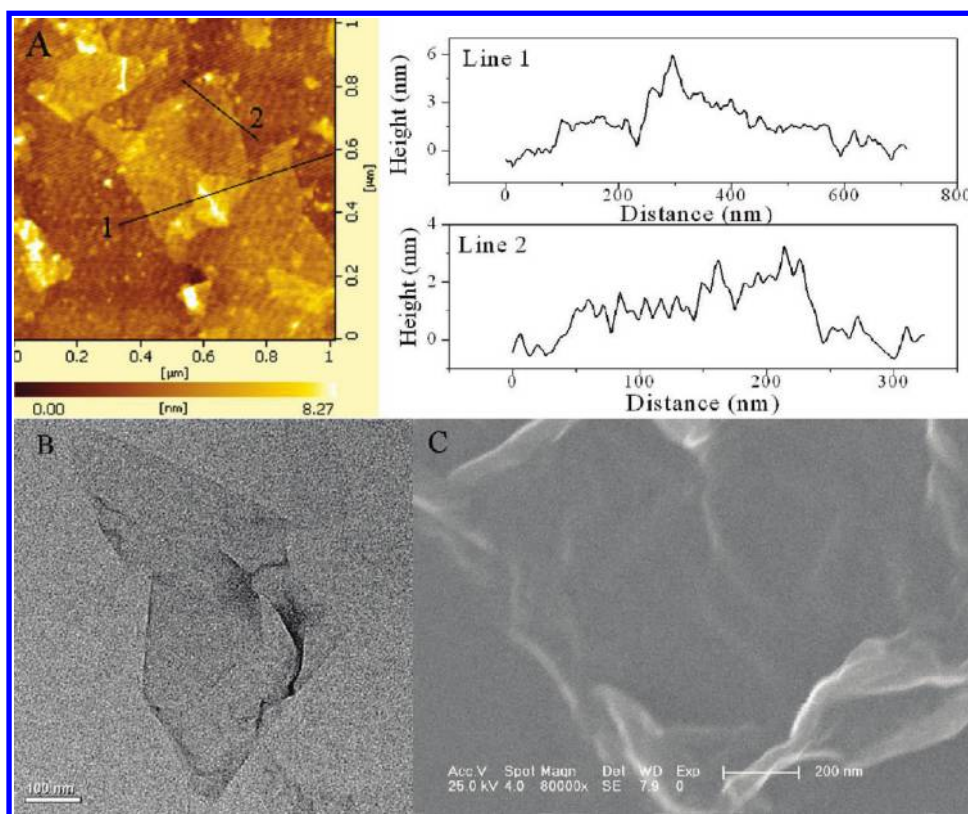


Figure 9. (A) Tapping-mode AFM image of GSCR self-assembled on a silicon wafer and (B) TEM and (C) SEM images of the GSCR composite. All samples were fabricated from the same GSCR aqueous solution after 100 days of storage.

solution might be that the CR molecules are firmly coupled to the graphene sheets by π - π stacking and that the $-\text{SO}_3\text{Na}$ groups of CR remain on the graphene sheets from one to another through electrostatic repulsion.

The conductivity of graphene sheets plays a very important role in their application in many fields. A GSCR film prepared by a vacuum filtration strategy (Figure S1) was used to measure its bulk conductivity by a four-probe method. The GSCR film have a bulk conductivity of $\sim 6850 \text{ S m}^{-1}$, which declines only slight comparing with that of GS films ($\sim 7200 \text{ S m}^{-1}$).¹⁸ The conductivity of GSCR is much superior to that of polymer-functionalized graphene sheets such as poly(sodium 4-styrenesulfonate)-modified graphene sheets, poly(vinyl pyrrolidone)-modified graphene sheets, and poly(2,5-bis(3-sulfonatopropoxy)-1,4-ethynylphenylene-alt-1,4-ethynylphenylene)-modified graphene sheets.⁴⁸ Thus, the resulting graphene sheets can be promisingly

applied in electronic devices because of their good conductivity, dispersibility, and stability.

3.3. Application of GSCR Composite. With the hybrid of CR, many soluble $-\text{SO}_3\text{Na}$ groups are introduced onto the surface of the GS composite. Unlike the sites of $-\text{COOH}$ groups concentrated at the edges of the GS composite,⁴⁹ the introduced $-\text{SO}_3\text{Na}$ groups can be uniformly distributed over the whole surface of the GSCR composite. Thus, these $-\text{SO}_3\text{Na}$ groups may provide many active sites on which to anchor other particles or molecules. As an example, the GSCR/Au composite was synthesized by simply mixing GSCR and Au-IL in an aqueous solution. Au nanoparticles are uniformly distributed over the whole surface of the GSCR composite (Figure 10). Moreover, the composition of the GSCR/Au composite is also confirmed by the XPS results (Figure S2). Although GS is also several hundreds nanometers with pleats (Figure S3A), when the Au nanoparticles

(48) Yang, H.; Zhang, Q.; Shan, C.; Li, F.; Han, D.; Niu, L. *Langmuir* **2010**, *26*, 6708–6712.

(49) Yuge, R.; Zhang, M.; Tomonari, M.; Yoshitake, T.; Iijima, S.; Yudasaka, M. *ACS Nano* **2008**, *2*, 1865–1870.

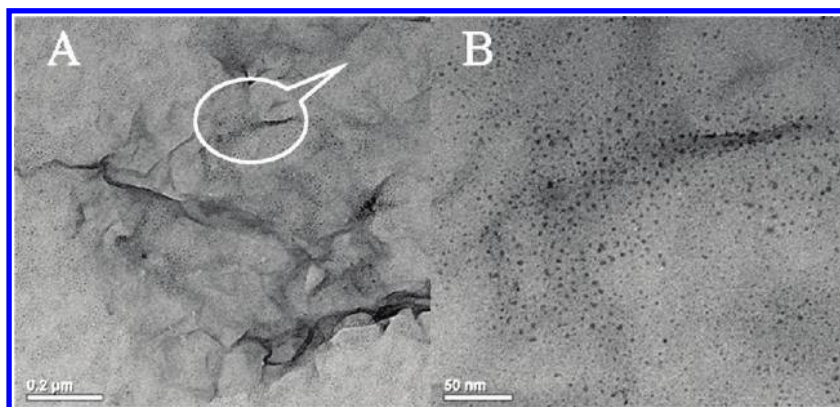


Figure 10. TEM images of the GSCR/Au composites.

decorated them, only a few dark spots of Au nanoparticles are observed at the edges and pleats of the GS substrate (Figure S3B). The GS/Au composite is formed through the electrostatic interaction between the $-\text{COOH}$ of GS and the $-\text{NH}_2$ of Au.⁴⁹ With the coupling of CR, the electrostatic force between $-\text{COOH}$ and $-\text{NH}_2$ is replaced by that between $-\text{SO}_3\text{Na}$ and $-\text{NH}_2$.⁴² Therefore, the GSCR composite easily anchor Au-IL onto graphene sheets because of the large number of $-\text{SO}_3\text{Na}$ groups.

4. Conclusions

The widely soluble GSCR composite was synthesized by coupling CR through noncovalent interactions. The resulting graphene sheets are completely dispersed in DMF, methanol, DMSO, ethanol, and water and partially dispersed in 10 other organic solvents. The Hansen solubility parameters are successfully used to elucidate the good dispersive properties of GSCR. The GSCR nanosheets still have an individual presence after 100 days of storage in water. Moreover, the GSCR films have a bulk conductivity of $\sim 6850 \text{ S m}^{-1}$, which is sufficient for many electrical applications. Finally, as an example, the GSCR/Au

composite was successfully synthesized because of the good solubility and stability of GSCR in water. Thus, the GSCR composite can be promisingly applied not only in producing graphene-based hybrid materials but also in electronic devices because of their unique properties.

Acknowledgment. This work was financially supported by the NSFC, China (nos. 20673109 and 20827004), the Chinese Academy of Sciences (nos. KGCX2-YW-231 and YZ200906), and the Bureau of Science & Technology of Changchun City (O660021F01).

Supporting Information Available: Details of the experimental procedure of synthesizing GO and GS, the Hansen solubility parameters of selected solvents, a digital photograph of the GSCR film used for conductivity measurements, TEM analysis of GS and GS/Au nanocomposites, and the XPS result for the GSCR/Au composite. This material is available free of charge via the Internet at <http://pubs.acs.org>.